

# Searching for hexagonal analogues of the half-metallic half-Heusler XYZ compounds

**Frederick Casper and Claudia Felser**

Institut für Anorganische Chemie und Analytische Chemie  
Johannes Gutenberg-Universität, Staudinger Weg 9, D-55099 Mainz, Germany.

**Ram Seshadri**

Materials Department and Materials Research Laboratory  
University of California, Santa Barbara, CA 93106, USA.

**C. Peter Sebastian and Rainer Pöttgen**

Institut für Anorganische und Analytische Chemie  
Westfälische Wilhelms-Universität Münster  
Correnstrasse 30, D-48149 Münster, Germany.

## Abstract.

The XYZ half-Heusler crystal structure can conveniently be described as a tetrahedral zinc blende YZ structure which is stuffed by a slightly ionic X species. This description is well suited to understand the electronic structure of semiconducting 8-electron compounds such as LiAlSi (formulated  $\text{Li}^+[\text{AlSi}]^-$ ) or semiconducting 18-electron compounds such as TiCoSb (formulated  $\text{Ti}^{4+}[\text{CoSb}]^{4-}$ ). The basis for this is that  $[\text{AlSi}]^-$  (with the same electron count as  $\text{Si}_2$ ) and  $[\text{CoSb}]^{4-}$  (the same electron count as GaSb), are both structurally and electronically, zinc-blende semiconductors. The electronic structure of half-metallic ferromagnets in this structure type can then be described as semiconductors with stuffing magnetic ions which have a local moment: For example, 22 electron MnNiSb can be written  $\text{Mn}^{3+}[\text{NiSb}]^{3-}$ . The tendency in the 18 electron compound for a semiconducting gap – believed to arise from strong covalency – is carried over in MnNiSb to a tendency for a gap in one spin direction. Here we similarly propose the systematic examination of 18-electron hexagonal compounds for semiconducting gaps; these would be the “stuffed wurtzite” analogues of the “stuffed zinc blende” half-Heusler compounds. These semiconductors could then serve as the basis for possibly new families of half-metallic compounds, attained through appropriate replacement of non-magnetic ions by magnetic ones. These semiconductors and semimetals with tunable charge carrier concentrations could also be interesting in the context of magnetoresistive and thermoelectric materials.

PACS numbers: 61.92.Fk, 71.20.-b, 75.50.Cc

## 1. Introduction

Half-metallic ferromagnets [1, 2], in contrast to more usual ferromagnets, are completely spin-polarized, possessing a gap in one spin direction at the Fermi energy  $E_F$ . Recent interest in the idea that solid state devices can function through manipulation of the spin of electrons [3, 4] has given rise to a wealth of research in the area of half-metals, which play an important rôle in spin-injection [5, 6]. An important fundamental question is what makes some ferromagnets half-metals, whilst others are not. This question has been addressed across large classes of materials such as the system  $\text{Fe}_{1-x}\text{Co}_x\text{S}_2$  [7, 8], in proposed epitaxial transition metal compounds with the zinc blende structure [9], in some chromium chalcogenide spinels [10, 11], and in the half-Heusler [1, 12, 13, 14, 15] and Heusler [16, 17, 18] compounds,  $\text{CrO}_2$  [19, 20] and some members of the colossal magnetoresistive manganites [21]. With the exception of the perovskite manganites, in all these different classes of half-metallic compounds, an interesting common theme that emerges is the existence of a band semiconductor that is quite proximal in terms of composition and electron count.

As an example, in  $\text{Fe}_{1-x}\text{Co}_x\text{S}_2$  perhaps the first series of compounds that were reported with integer moments on the magnetic substituents [22], the starting point is semiconducting  $\text{FeS}_2$  whose empty  $e_g$  band is populated through Co substitution. Similarly, the basis for zinc blende half-metals [9, 23] is the replacement of cations in a semiconductor with magnetic ions: Half-metallic zinc blende CrAs can be considered the magnetic analogue of GaAs, or perhaps even more appropriately, as the magnetic analogue of zinc blende ScAs, with the semiconducting gap being retained in the magnetic compound albeit in one spin direction. Similar analogies can be drawn for systems such as rutile  $\text{CrO}_2$  [19, 20].

One of the best studied systems of half-metals are the half-Heusler compounds XYZ exemplified by  $\text{MnNiSb}$  [1]. Whangbo and coworkers pointed [13] out that the 18 electron half-Heusler compounds must be non-magnetic and semiconducting. Recently, Galanakis [12] has placed these half-Heusler compounds on a firm theoretical footing, suggesting that in the half-metallic compositions, the magnetic moment obtained from the saturation magnetization  $M$ , per formula unit, should vary as  $M = Z_t - 18$  where  $Z_t$  is the total number of valence electrons. Some of us [14] have examined the role that covalency plays and have proposed that the half-Heusler compounds are both structurally and electronically best treated as an  $X$  ion stuffing a zinc blende  $YZ$  structure. When the  $X$  ion is nonmagnetic and  $Z_t = 18$ , the compound is a band semiconductor. If  $X$  is magnetic and  $Z_t \neq 18$ , such as in  $\text{MnNiSb}$  with  $Z_t = 22$ , the compound is a half-metallic ferromagnet, with, in the case of  $\text{MnNiSb}$ , a magnetic moment of  $4\mu_B$  per formula unit.

In this contribution, we ask the following question: If XYZ stuffed zinc blende compounds with  $Z_t = 18$  are semiconducting, can similar 18 electron semiconductors be found amongst 18 electron XYZ stuffed wurtzites, given that wurtzite and zinc blende are simply stacking variants of one another with very similar topologies and

hence bonding patterns. We suggest the answer is yes, and examine different closely related hexagonal XYZ compounds: ScCuSn, LaCuSn and YCuSn. We use this to propose related magnetic compounds that would potentially comprise a novel class of half metallic XYZ compounds with hexagonal crystal structure.

Hexagonal XYZ compounds with cerium, europium, ytterbium, and uranium as the  $X$  atom have been investigated in the last twenty years in light of their unusual properties. Examples include valence-fluctuations in EuPtP [24], the Verwey type transition in EuNiP [25], intermediate-valent YbCuAl [26], the 10 K ferromagnet CeAuGe [27], the Kondo system CePtSn [28], and the heavy fermion material CePtSi [29]. CeRhAs is a Kondo semiconductor in the stuffed wurtzite structure, which undergoes an electronic transition at high temperature and pressure into a metallic phase simultaneously with a structural transition into the TiNiSi structure [30]. The rare-earth–Pd–Sb system is particularly interesting since CePdSb is a 17 K Kondo ferromagnet with a resistance minimum, while many members of this series prepared with other magnetic rare-earths are antiferromagnetic [31]. The tunability of electronic structure and the charge carrier density in this structure type make the compounds of this structure type interesting for magnetoresistance effects [32, 33], and it is likely that they would be a fertile class of thermoelectric compounds as well.

## 2. Computational methods

Density functional theory-based electronic structure calculations reported here were performed using the linear muffin tin orbital method [34] within the local spin density approximation. The crystal structure inputs for the calculations were obtained from experimental data in the literature, except when hypothetical structures are considered. Crystal orbital Hamiltonian populations (COHP) [35] and the electron localization function (ELF) [36, 37] were used to obtain insights into bonding in the title compounds, respectively, in terms of the strengths of individual bonds, as well as in real space.

## 3. Results and discussion

### 3.1. Crystal structures of the hexagonal compounds $XCuSn$

A huge variety of the equiatomic intermetallic compounds XYZ ( $X$  = rare earth,  $Y$  = late transition metal element,  $Z$  = main group element) crystallize in structure types related to the  $AlB_2$  family. The ordered superstructures crystallize in the LiGaGe, NdPtSb, and ZrBeSi type structures. The late transition metals and the main group elements form  $Y_3Z_3$  hexagons, which are connected in a two dimensional honeycomb network. Disorder between the transition metals and the main group elements leads to the pseudobinary structure types like  $AlB_2$ ,  $Ni_2In$ , or  $CaIn_2$ . The layers can be planar like in graphite (found in the ZrBeSi and  $AlB_2$  types), weakly puckered (NdPtSb type) or strongly puckered with short interatomic distances between the layers leading to a wurtzite-related structure with a three dimensional network (LiGaGe type). Compared

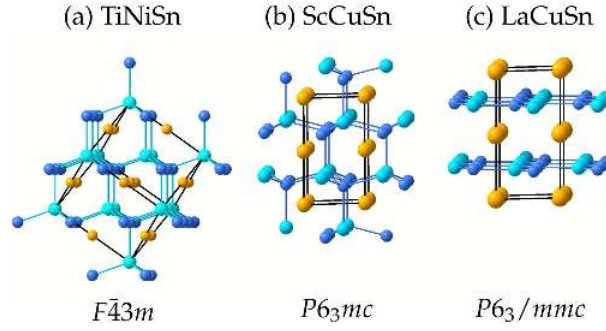


**Figure 1.** (Color online) Crystal structures of (a) the half-Heusler compound TiNiSn, (b) the stuffed wurtzite ScCuSn with the LiGaGe structure, and (c) LaCuSn, in the ZrBeSi structure type. The structures are depicted in a manner that highlights respectively, the zinc-blende NiSn, the wurtzite CuSn, and the “decorated graphite” CuSn networks. The orange spheres are respectively Ti, Sc, and La. Light and dark blue spheres represent (Ni/Cu) and Sn.

| compound                | Space Group | $a$ (Å) | $c$ (Å) | $c/a$ | $z(\text{Cu})$ | $z(\text{Sn})$ |
|-------------------------|-------------|---------|---------|-------|----------------|----------------|
| LaCuSn                  | $P6_3/mmc$  | 4.583   | 8.173   | 1.783 | 0.75           | 0.25           |
| YCuSn                   | $P6_3mc$    | 4.513   | 7.274   | 1.612 | 0.8148         | 0.2318         |
| ScCuSn                  | $P6_3mc$    | 4.388   | 6.830   | 1.557 | 0.82545        | 0.22914        |
| hypothetical structures |             |         |         |       |                |                |
| LaCuSn [LiGaGe]         | $P6_3mc$    | 4.583   | 8.173   | 1.783 | 0.78           | 0.22           |
| LaCuSn [wurtzite]       | $P6_3mc$    | 5.005   | 8.173   | 1.633 | 0.8125         | 0.1875         |

**Table 1.** Crystal structures of the compounds whose electronic structures are described in this contribution.  $X$  (Sc, Y, La) at  $(0,0,0)$ , Cu at  $(\frac{2}{3}, \frac{1}{3}, z(\text{Cu}))$  and Sn at  $(\frac{1}{3}, \frac{2}{3}, z(\text{Sn}))$ . The first three experimental crystal structures are taken from reference [38].

to the compounds with the stuffed zinc blende structure, namely the  $C_{1b}$  half-Heusler compounds, the LiGaGe structure type which is the focus of this contribution has a free lattice parameter, the  $c/a$  ratio, which should be 1.633 for the ideal hexagonal wurtzite structure. Beside the variable  $c/a$  ratio, the free  $z$  parameter of the  $2b$  positions (see table 1) allows different degrees of puckering of the hexagons leading to structures that can vary almost continuously from three dimensional to quasi-two dimensional, with anticipated changes in electronic properties. Due to this reduction in symmetry in comparison with the half-Heusler compounds, a large variety of different structure types are possible as described above. The different superstructures are related via group-subgroup relations as recently reviewed [39]. The bonding features in such materials have been discussed in several overviews [40, 41, 42, 43, 44, 45]. Of the compounds discussed here, ScCuSn and YCuSn are examples for the puckered LiGaGe-type structure, whereas LaCuSn is an example of a planar  $[\text{YZ}]^{3-}$  (here  $\text{CuSn}^{3-}$ ) network [38]. CeCuSn is dimorphic with different degrees of puckering in the low- and high-temperature modifications [46].

Figure 1 compares the crystal structure of a typical cubic half-Heusler compound, (a)  $F\bar{4}3m$  TiNiSn, with the crystal structures of two variants of the hexagonal XYZ compounds discussed here:  $P6_3mc$  ScCuSn [38], crystallizing in the LiGaGe type structure and the planar  $P6_3/mmc$  LaCuSn [38]. TiNiSn is displayed with bonds connecting the zinc blende network of Ni and Sn. The Ti atoms stuff the (6+4)-coordinate voids of the zinc blende structure. The structure is displayed with the [111] direction pointing up in the plane of the page, in order to emphasize the ABC stacking each of the three *fcc* substructures of the half-Heusler structure. ScCuSn can be thought of as comprising a  $\text{Sc}^{3+}$  ion stuffing a wurtzite  $[\text{CuSn}]^{3-}$  substructure where the number of electrons is 18 ( $d^0 + d^{10} + s^2 + p^6$ ). LaCuSn is also a 18 valence electron compound which crystallizes in the ZrBeSi-type structure. In this structure type, compounds with usually 18 valence electrons are found with some exceptions.

From the described electron count of these 18 electron compounds, we would expect closed shell species similar to the 18-electron half-Heusler compounds: Non-magnetic, and semiconducting, at least for ScCuSn. In LaCuSn the  $[\text{CuSn}]^{3-}$  honeycomb network adopts a planar graphite type layer. This structural change from ScCuSn *via* YCuSn to LaCuSn is reflected in the  $c/a$  ratio and the  $z$  parameter, listed in table 1. The  $c/a$  ratio decreases with an increase of the puckering.

### 3.2. Electronic structures of the hexagonal compounds $\text{XCuSn}$

We have examined the  $\text{XCuSn}$  compounds using LMTO calculations. The experimental lattice constants and experimental  $z$ -parameters were employed in the input crystal structures to investigate the influence of puckering of the honeycomb  $Y_3Z_3$  networks on the electronic structure. Additionally, calculations were performed for LaCuSn in two hypothetical structures described in table 1: The LiGaGe structure with experimental lattice parameters and hypothetical  $z$  parameters which result in puckered  $\text{Cu}_3\text{Sn}_3$  honeycombs, and an ideal wurtzite structure with the experimental  $c$  parameter, and  $a$  and  $z$  chosen so that the ideal wurtzite structure is obtained ( $c/a = 1.633$ ). In this ideal structure, all  $\text{CuSn}_4$  and  $\text{SnCu}_4$  tetrahedra are regular.

In the three panels of figure 2, we compare the densities of states (DOS) near the Fermi energy  $E_F$  for LaCuSn, YCuSn, and ScCuSn calculated for the experimental structures. We see trends in the electronic structure as the CuSn networks in these structures are increasingly puckered. All compounds have a noticeable pseudo band gap at  $E_F$ , with a more pronounced gap in the more puckered Y and Sc compounds. Projections of the densities of state on the different orbitals (not displayed) reveal that the valence band has mainly Sn *p* character. The Sn *s* states are separated by a gap from the valence band at around  $-8\text{ eV}$ . The bottom of the valence band is built from Sn *p* states. Cu *d* states lead to spikes in the electronic structure around  $-3.5\text{ eV}$  (ScCuSn) or  $-3\text{ eV}$  (LaCuSn). The Cu *d* bands are very flat with an over all dispersion of  $0.5\text{ eV}$ . In the three-dimensional compound ScCuSn all Sn *p* states contributes to the states below and above the copper states. In two dimensional LaCuSn, the bottom of the

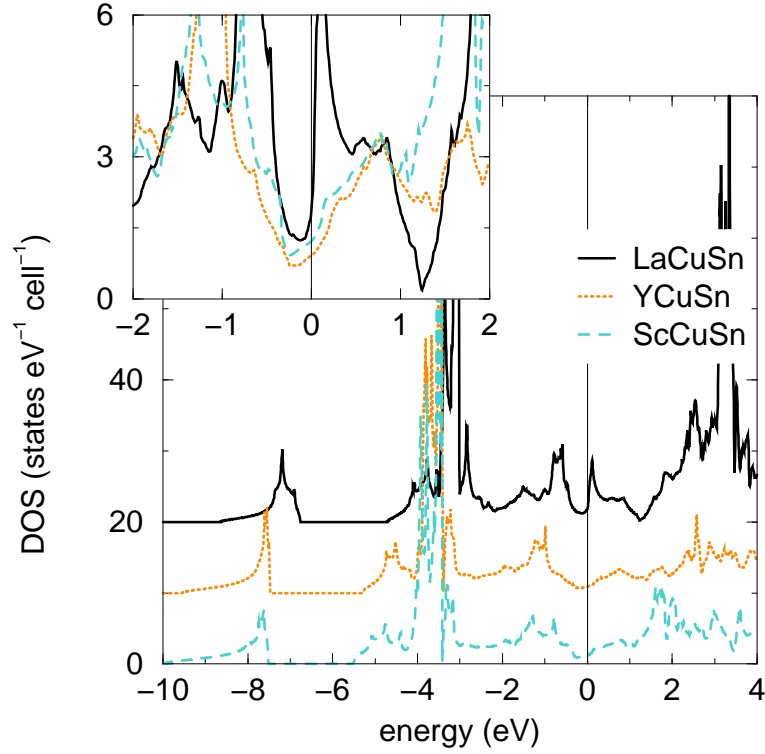


**Figure 2.** (Color online) Total densities of state obtained from LMTO calculations on the experimental crystal structures of LaCuSn, YCuSn, and ScCuSn. The DOS are offset on the ordinate for clarity. The inset shows the DOS of the three compounds in a region close to  $E_F$ . These data are not offset.

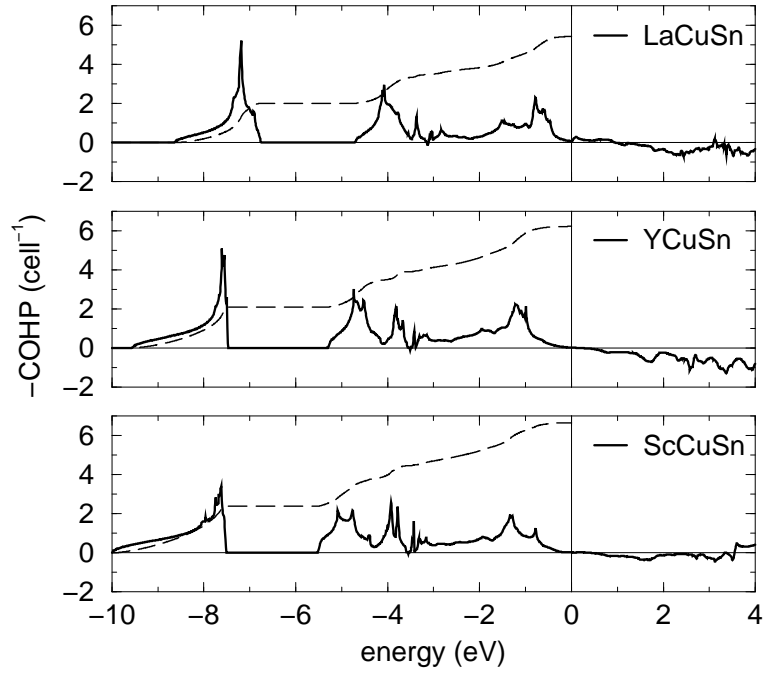


**Figure 3.** Crystal orbital Hamiltonian populations (COHPs) of the Cu-Sn interaction in the three compounds, LaCuSn, YCuSn, and ScCuSn.

valence states around  $-4\text{ eV}$  has pronounced Sn  $p_z$  character, whereas the top of the valence band is mainly built from Sn  $p_x$  and  $p_y$  states. Sc or rare-earth d states form the conduction band with a band width around  $5\text{ eV}$  and have a small contribution to the Sn p states below  $E_F$ . From the density of states we can conclude that a description of the compound as  $X^{+3}$  ion stuffing a wurtzite or “decorated graphite”  $[\text{CuSn}]^{3-}$  substructure is appropriate. The total DOS of these hexagonal compounds look very similar to those of the half-Heusler compounds [14], with some differences in the projected densities due to the different electronegativities of the constituent elements.

The similarities and differences in the electronic structure of the three compounds are further emphasized through an analysis of the Cu-Sn COHPs of the three stannides displayed in figure 3. Cu-Sn is the main bonding interaction in these compounds and bonding and antibonding states are separated by the Fermi energy. The dashed line in this figure is an integration of the COHP up to the  $E_F$ , yielding a number that is indicative of the strength of the bonding. The extents of the bonding and the antibonding states of the Cu-Sn COHPs is slightly larger in the puckered compounds compared to the planar LaCuSn. Integrating the COHPs, we find that the strongest bonding interaction is in the planar LaCuSn. The planar Cu-Sn layers seem to lead to a stronger Cu-Sn interaction than the puckered Cu-Sn layers. However, the total bonding interaction seems to be stronger in the puckered compounds. Cu-Sn interactions are nonbonding around and above  $E_F$  and therefore do not contribute to the states around  $E_F$ . In YCuSn and ScCuSn, the other pairwise interactions are significant smaller: The X-Cu interaction is only 10%, and the X-Sn interaction is around 20% of the Cu-Sn interaction. The X-Cu interaction is bonding below  $E_F$  and small and slightly bonding above  $E_F$ . We can conclude that the bonding interactions in the hexagonal compounds ScCuSn and YCuSn are similar to what are found in the half Heusler compounds [14]. A much stronger La-Cu interaction is found in the planar compound LaCuSn (not shown). The La-Cu interaction leads to a strong bonding interaction leading to the high density of states peak slightly above  $E_F$ . The La-Sn states build the top of the valence band and are responsible for reducing the magnitude of the pseudogap in this compound. It is clear from this discussion that YCuSn and ScCuSn are electronically well described as stuffed wurtzite compounds, with pseudogaps at  $E_F$  between the bonding and antibonding states

### 3.3. The influence of puckering on the band structure and the electron localization function

The fact that the puckering of the Cu-Sn layer seems to be responsible for the metallic or semimetallic behaviour of hexagonal 18 electron compounds has motivated us to look more close on the influence of the puckering on the band structure and the gap of these compounds. Here we discuss the band structure of LaCuSn in the experimental structure and in the hypothetical LiGaGe-type and the wurtzite-type structures. Figure 4 displays the band structure of (a) LaCuSn with the experimental ZrBeSi-type structure, (b)

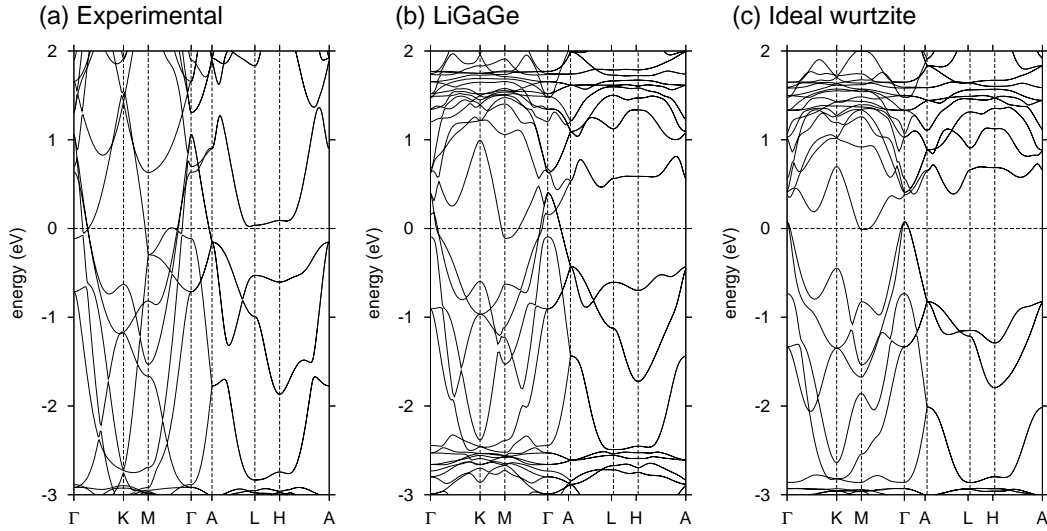


**Figure 4.** Band structures of experimental and hypothetical LaCuSn structures.

hypothetical LaCuSn with the LiGaGe-type and (c) LaCuSn with the ideal wurtzite-type structure. These structures are described in table 1. LaCuSn in its experimental structure is clearly a metal in the  $\Gamma - K - M - \Gamma$  direction and shows a gap of nearly 0.3 eV along the direction at the surface of the Brillouin zone  $A - L - H - A$ . In the LiGaGe structure the compound would be a semimetal due to the dipping of the conduction band at the M point and the valence band at the  $\Gamma$  point. In the hypothetical wurtzite structure LaCuSn becomes semiconducting. A closer view on the bands and their eigenvectors around  $E_F$  shows that the metallicity is due to an overlap between the conduction band with mainly La  $d_{x^2-y^2}$  and  $d_{3z^2-1}$  character and the Sn  $p_x$  and  $p_y$  valence band. Symmetry induces a metal to semiconductor transition by going from the ZrBeSi-type structure to the LiGaGe-type structure. For the experimental structure the La band dips below the Fermi energy at the M point with mainly  $d_{3z^2-1}$  character and the Sn  $p_x$  and  $p_x$  bands cross  $E_F$  around  $\Gamma$ . It is surprising that the overall band dispersion in the planar layers is much higher compared to the puckered layers. However a detailed look on the eigenvectors lead to a simple explanation. In case of the planar Cu-Sn layers the bands with Sn  $p_x$  and  $p_y$  contribution have a larger dispersion compared to the puckered layers. The strength of this interaction depends on the bonding distance and the effective overlap of the orbitals, both is stronger in case of the planar layers. The strong sigma type bonding interaction between Sn and Cu pushes the valence band above the Fermi level at the  $\Gamma$  point. The conduction band which is derived from La  $d_{3z^2-1}$  displays a dispersion of nearly 2 eV and dips below  $E_F$  along the  $\Gamma$  to M direction.

The same band of the puckered structures, the La  $d_{3z^2-1}$  band, has a much smaller dispersion of 0.5 eV and touches the Fermi energy slightly at the M point. The most important point is that the degeneracy at the M point between the La  $d_{3z^2-1}$  and the Sn  $p_x$  band is lifted by reducing the symmetry from the  $P6_3/mmc$  to  $P6_3mc$ , which renders the opening of the gap possible in the LiGaGe-type and wurtzite-type structure.



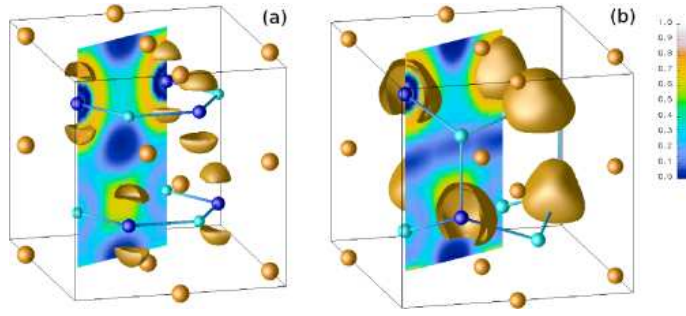


**Figure 5.** (Color online) Electron localization functions (ELFs) of the valence electrons of LaCuSn in (a) the experimental crystal structure and in the (b) hypothetical wurtzite structure. The ELF isosurface is displayed for a value of 0.75.

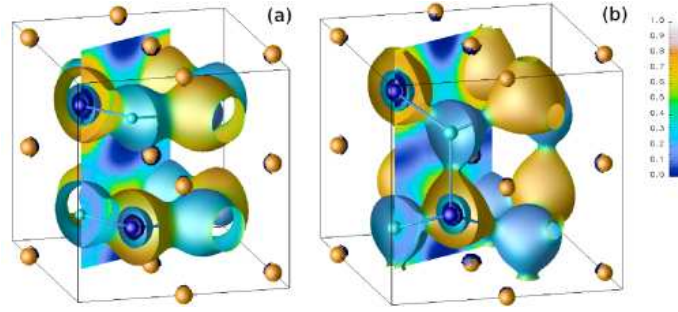


**Figure 6.** (Color online) Electron density isosurfaces plotted for values of  $0.025 \text{ e}\text{\AA}^{-3}$  for LaCuSn in (a) the experimental crystal structure and in the (b) hypothetical wurtzite structure. The electron density is colored according to the degree of localization.

In a manner similar to the half-Heusler compounds, the hexagonal compounds display an indirect gap, here between the  $\Gamma$  and the M point.

By puckering the structure in going from the graphite type structure via LiGaGe to the ideal wurtzite-type structure the overlap between the conduction and the valence band becomes smaller and the symmetry is reduced. The compounds with LiGaGe structure can show semiconducting or semimetallic behaviour, what is experimentally and theoretically found for CePdSb [47] and CeRhAs [30]. Introducing  $f$ -elements like Gd lead to half metallic ferromagnets for example in GdPdSb [48].

Real space visualization of the electronic structure employed the electron localization function (ELF) for LaCuSn in figure 5(a) for the experimental ZrBeSi-type and in figure 5(b) for the hypothetical wurtzite structure. The value of localization runs from 0 (no localization, deep blue) to 1 (high localization, white). The isosurface of 0.75 is displayed here. The colored map in the background is the ELF shown on a  $(11\bar{2}0)$  plane to visualize the bonding interaction along the Cu-Sn network. For the ZrBeSi type structure figure 5(b) the Sn p electrons perpendicular to planar Cu-Sn layer in are strongly localized. These p states interact strongly with La  $d_{3z^2-1}$  states with the layer, and are responsible for closure of the gap and the metallicity of the compound. In figure 5(b), we find clear evidence for highly covalent and three-dimensional bonding

between Cu (cyan) and Sn (blue) in the wurtzite substructure of the wurtzite-type LaCuSn. As observed in the half Heusler compounds, the localization is closer to the more electronegative Sn atom [14].

The valence charge densities displayed in figures 6(a) and (b) are again very similar to the valence charge densities of the half Heusler compounds [14]. Because of the filled d shells on Cu it forms large nearly spherical blobs around that atom, visualized for a charge density of  $0.025 e\text{\AA}^{-3}$ . We find that these blobs of charge are pulled out into four strongly localized (as seen from the colouring) lobes arranged tetrahedrally and facing Sn in (b), whilst in the LiGaGe structure, the bonding interaction in the third dimension is removed, leading to three lobes arranged trigonal in the plane and facing the Sn in the plane.

## 4. Conclusion

We have carried out a systematic examination of XYZ compounds with hexagonal structures: LaCuSn, YCuSn, and ScCuSn, and demonstrated that 18-electron compounds can become semiconductors depending on the degree of puckering of the  $[\text{CuSn}]^{3-}$  substructure. We demonstrate that the most instructive way of considering these systems is to think of them as being built up of a wurtzite [YZ] framework that is stuffed with the electropositive X. An effective strategy for new half-metals, in analogy with half-Heusler half-metals, would be to stuff these wurtzite-derived structures with magnetic ions.

## Acknowledgments

CPS, HCK, CF, and RP acknowledge support from the DFG within the priority programme SPP 1166 *Lanthanoidspezifische Funktionalitäten in Molekül und Material*. CPS also acknowledges the NRW Graduate School of Chemistry for a PhD stipend. RS acknowledges the US NSF for support through a Career Award (DMR04-49354).

- [1] de Groot R A, Mueller F M, Engen P G v and Buschow K H J 1983 *Phys. Rev. Lett.* **50** 2024–2027
- [2] Felser C, Fecher G and Balke B 2007 *Angew. Chem. Intl. Edn.* **46** 668
- [3] Wolf S A, Awschalom D D, Buhrman R A, Daughton J M, von Molnar S, Roukes M L, Chtchelkanova A Y and Treger D M 2001 *Science* **294** 1488
- [4] Žutić I, Fabian J and Das Sarma S 2004 *Rev. Mod. Phys.* **76** 323
- [5] Pickett W S and Moodera J S 2001 *Phys. Today* **54** 34
- [6] Grünberg P 2001 *Phys. Today* **54** 31
- [7] Mazin I I 2000 *Appl. Phys. Lett.* **77** 3000–3002
- [8] Ramesha K, Seshadri R, Ederer C, He T and Subramanian M A 2004 *Phys. Rev. B* **70** 214409
- [9] Pask J E, Yang L H, Fong C Y, Pickett W E and Dag S 2003 *Phys. Rev. B* **67** 224420
- [10] Horikawa J I, Hamajima T, Ogata F, Kambara T and Gondaira K I 1982 *J. Phys. C: Solid State Physics* **15** 2613–2623
- [11] Park M S, Kwon S K, Youn S J and Min B I 1999 *Phys. Rev. B* **59** 10018–10024
- [12] Galanakis I, Dederichs P H and Papanikolaou N 2002 *Phys. Rev. B* **66** 134428
- [13] Jung D, Koo H J and Whangbo M H 2000 *J. Mol. Struc: THEOCHEM* **527** 113–119
- [14] Kandpal H C, Felser C and Seshadri R 2006 *J. Phys. D: Appl. Phys.* **39** 776–785

- [15] Köhler J, Deng S, Lee C and Whangbo M H 2007 *Inorg. Chem.* **46** 1957
- [16] Palmstrom C 2003 *MRS Bull.* **28** 725–728
- [17] Galanakis I, Dederichs P H and Papanikolaou N 2002 *Phys. Rev. B* **66** 174429
- [18] Block T, Felser C, Jakob G, Ensling J, Mühling B, Gütlich P and Cava R J 2003 *J. Solid State Chem* **176** 646
- [19] Sorantin P I and Schwarz K 1992 *Inorg. Chem.* **31** 567–576
- [20] Mazin I I, Singh D J and Ambrosch-Draxl C 1999 *Phys. Rev. B* **59** 411–418
- [21] Pickett W E and Singh D J 1996 *Phys. Rev. B* **53** 1146–1160
- [22] Jarrett H S, Cloud W H, Bouchard R J, Butler S R, Frederick C G and Gillson J L 1968 *Phys. Rev. Lett.* **21** 617–620
- [23] Galanakis I and Mavropoulos P 2003 *Phys. Rev. B* **67** 104417
- [24] Lossau N, Kierspel H, Langen J, Schlabit W, Wohlleben D, Mewis A and Sauer C 1989 *Z. Phys. B* **74** 227
- [25] Ksenofontov V, Kandpal H C, Ensling J, Waldeck M, Johrendt D, Mewis A, Gütlich P and Felser C 2006 *Europhys. Lett.* **74** 672
- [26] Pöttgen R, Johrendt D and Kußmann D 2001 *Handbook on the Physics and Chemistry of Rare Earths, North-Holland/Elsevier, Amsterdam* **32** 453
- [27] Pöttgen R, Borrmann H and Kremer R K 1996 *J. Magn. Magn. Mater.* **152** 192
- [28] Riecken J F, Heymann G, Soltner T, Hoffmann R D, Huppertz H, Johrendt D and Pöttgen R 2005 *Z. Naturforsch.* **60b** 825
- [29] Lee W H and Shelton R N 1987 *Phys. Rev. B* **35** 5369
- [30] Umeo K, Masumori K, Sasakawa T, Iga F, Takabatake T, Ohishi Y and Adachi T 2005 *Phys. Rev. B* **71** 064110
- [31] Malik S K and Adroja D T 1991 *J. Magn. Magn. Mater.* **102** 42–46
- [32] Casper F, Ksenofontov V, Kandpal H C, Reiman S, Shishido T, Takahashi M, Takeda M and Felser C 2006 *Z. Anorg. Allg. Chem.* **632** 1273
- [33] Pierre J and Karla I 2000 *J. Magn. Magn. Mater.* **217** 74
- [34] Jepsen O and Andersen O K 2000 The STUTTGART TB-LMTO-ASA program version 47
- [35] Dronskowski R and Bloechl P E 1993 *J. Phys. Chem.* **97** 8617–8624
- [36] Becke A D and Edgecombe K E 1990 *J. Chem. Phys.* **92** 5397–5403
- [37] Silvi B and Savin A 1994 *Nature* **371** 683–686
- [38] Sebastian C P, Fehse C, Eckert H, Hoffmann R D and Pöttgen R 2006 *Solid State Sci.* **8** 1386
- [39] Hoffmann R D and Pöttgen R 2001 *Z. Kristallogr.* **216** 127
- [40] Pöttgen R, Borrmann H, Felser C, Jepsen O, Henn R, Kremer R and Simon A 1996 *J. Alloys. Compd.* **23** 170
- [41] Nuspl G, Polborn K, Evers J, Landrum G A and Hoffmann R 1996 *Inorg. Chem.* **35** 6922
- [42] Landrum G A, Hoffmann R, Evers J and Boysen H 1998 *Inorg. Chem.* **37** 5754
- [43] Bojin M D and Hoffmann R 2003 *Helv. Chim. Acta* **86** 1653
- [44] Bojin M D and Hoffmann R 2003 *Helv. Chim. Acta* **86** 1683
- [45] Gaudin E, Chevalier B, Heying U, Rodewald C and Pöttgen R 2005 *Chem. Mater.* **17** 2693
- [46] Sebastian C P, Rayaprol S, Hoffmann R D, Rodewald U C, Pape T and Pöttgen R 2007 *Z. Naturforsch.* **62b** 647
- [47] Ślebarski A 2006 *J. Alloys Compd.* **423** 15
- [48] Casper F, Kandpal H C, Fecher G H and Felser C 2007 *J. Phys. D: Appl. Phys.* **40** 3024